Earthq Eng & Eng Vib (2020) 19: 583-595 **DOI**: https://doi.org/10.1007/s11803-020-0582-x

Influence of scattering of SH-waves in dynamic interaction of shear wall with soil layers

Shashi Kumar[1†, 2‡, 3§] and Swapan Kumar Chakraborty[3*]

1. *Department of Mathematics, Sarala Birla University, Ranchi 835103, India*

2. *Department of Applied Mathematics, Cambridge Institute of Technology, Ranchi 835103, India*

3. *Department of Mathematics, Birla Institute of Technology, Mesra, Ranchi 835215, India*

Abstract: The dynamic soil-structure interaction of a shear wall embedded in elastic isotropic and homogeneous soil layers underlain by bedrock, subjected to SH waves, is modeled in the present article. The soil layers consist of irregular interfaces and it has been shown that the scattering due to the roughness of the layers has significant effect on the displacement of both the foundation and the shear wall. To demonstrate the phenomena indirect boundary element method (IBEM) has been used on the basis of its validation in previous problems of similar type. The system response is compared with the analytical solution of the same type of model for vertically propagating incident SH waves. It is observed that for the low frequency of wave, displacement is abruptly high, and as a result the combination of shear wall and foundation perceives resonance. The thickness of the soil layer, mass of the shear wall, stiffness of the bedrock and the soil layers all affects the system frequency and displacement.

Keywords: soil-layers; semi-circular foundation; shear wall; scattering

1 Introduction

Soil-structure interaction plays an important role in structural dynamics. In earthquake engineering, many problems have dealt with the study of soil-structure interaction and its influence on the structural response due to seismic waves. In most practical engineering applications, depending on the soil conditions and structural type, the foundations are partially or totally embedded in the ground and it is found that the surrounding soil greatly alters their static and dynamic response. This became part of the attraction to studying the effect of different types of foundations and the surrounding soil.

The response of an infinitely-long elastic shear wall erected on a rigid semi-cylindrical foundation was studied for vertically incident SH waves by using analytical method (Luco, 1969). Later on this was generalized to arbitrary incidence of S waves (Trifunac, 1972). These solutions later were extended to 2-D semi-elliptical foundations (Wong and Trifunac, 1974), 3-D foundation (Lee, 1979), and to torsional response (Luco, 1976; Apsel and Luco, 1976). Analytical solutions were discussed for in-plane 2-D response due to incident P, SV, and Rayleigh waves by approximating the ground surface as a circular arc with very large radius (Todorovska, 1993). Next the model was used to study the difference of soil-structure interaction in dry and water saturated sits for poroelastic half-space (Todorovska and Rjoub, 2006a and 2006b). Soil-structure interaction is also studied by Lee and Luo (2014) for shallow rigid circular foundations due to Plane SH waves from far-field earthquakes.

The use of analytical methods is restricted to simple foundations and homogeneous half-space. To study more complex structural systems, numerical methods such as the finite element method (FEM) and the boundary element method (BEM) were also developed. FEM requires the use of special transmitting boundaries or infinite elements, which may lead to inaccuracy because of the difficulty of satisfying the boundary condition at infinity. To solve the problem of inaccuracy artificial boundaries have been considered. An artificial viscous boundary has been introduced to study the vertical impedance function and the effective input motion of a circular surface foundation and an embedded column foundation in homogeneous half-space (Luco and Wong, 1987). The impedance function of surface or embedded foundations in a layered half-space has been analyzed to examine the effects of layer depth, embedment depth and

Correspondence to: Shashi Kumar, Dept. of Mathematics,Sarala Birla University, Birla Knowledge City, Mahilong, Purulia Road, Ranchi 835103, Jharkhand, India
Tel: +918757669305
E-mail: shashik2552@gmail.com
[†]Assistant Professor; [‡]Ex-Assistant Professor; [§]Ex-Phd Candidate; [*]Professor and Ex-Head

Received November 1, 2018; **Accepted** June 25, 2019

Poisson′s ratio by setting consistent boundary conditions (Kausel *et al*., 1975; Tassoulas and Kausel, 1983). An iterative transmitting boundary has been introduced for the dynamic soil structure interaction of a nuclear power plant in half-space (Liao *et al*., 1984; Liao, 1999). There are more examples of artificial boundaries which include non-reflecting boundaries (Smith, 1974) and absorbing boundaries (Clayton and Engquist, 1977; Engquist and Majda, 1977; Higdon, 1986). Another method known as the scaled boundary finite element method (SBFEM) also has been used to study dynamic structure-foundation-soil interaction by Li *et al*. (2013).

The boundary element method (BEM) only discretizes the boundary of the definition domain. It is different from the discretization of total continuum and uses functions satisfying the governing equation to approximate boundary conditions. It does not need artificial boundaries because it uses Green′s functions, which that automatically satisfy the radiation conditions at infinity. A Green′s function of a load uniformly distributed on an inclined line has been used to calculate impedance functions of embedded foundations (Wolf and Darbre, 1984a and 1984b). Studies for 2-D and 3-D foundations, in homogeneous or layered half-space, using Green′s functions of point loads and a non singular integral approach have been presented (Luco and Wong, 1987; de Barros and Luco, 1995; Manolis and Beskos, 1988; Sbartai and Boumekik, 2008; Messioud *et al*., 2016). It has been shown that compliant bedrock influences the impedance function and the number of peaks in the frequency domain and that the amplitudes of peaks depend on the thickness of the soil deposit (Abascal and Dominguez, 1986; Japon *et al*., 1997).

Formers carried work concerning the effect of the site characteristics on dynamic soil-structure interaction but it is not characterized for many physical properties of the site, such as soil layers of irregular interfaces. In this literature, Liang *et al*. (2013) carried the effort by using the indirect boundary element method (IBEM) for the effect of soil layer over bedrock in the model of shear wall with semi-circular rigid foundation. The soil-layer is described as a homogeneous and isotropic medium and is assumed to consist that it consists of a finite number of layers with plane interfaces in between the bedrock and the free ground surface.

In contrast to the model considered by the previous researchers (Liang *et al*., 2013), the ensuing model consists of irregular layers, as in reality this type of layers exists beneath the earth surface. So, it is imperative to study the present model′s conformance to reality. In this paper there is an indirect boundary element method (IBEM) to evaluate the influence of site with soil layer consisting of a finite number of irregular faced sub layers in between the bedrock and the free ground surface. This problem seems to be more practical and scattering of SH waves in multilayered media with irregular interfaces has many applications in dynamic soil-structure interaction. The methodology here uses Green′s function (Liang *et al*., 2013; Wolf, 1985; Liang and Ba, 2007; Aki and Richards, 1980; Ding and Dravinski, 1996; Ba *et al*., 2018; Wang *et al*., 2017) to explain dynamic response of the model and the result is compared with de Barros and Luco (1995), Liang *et al*. (2013), and Trifunac (1972) to see the effect of scattering of waves in soil-structure interaction and vibration of foundation and shear wall. It is found that the scattering of SH waves due to irregular soil interfaces has considerable influence in the motion of shear wall and the soil-structure interaction.

2 Methodology

2.1 Model

The model consists of a shear wall with rigid semi-circular foundation embedded beneath the elastic layers of soil overlaying elastic half-space (bedrock). The interfaces between the layers are assumed to be irregular but sufficiently smooth without sharp corners. Both the soil layers and bedrock are homogeneous and isotropic. As in Fig. 1, the total thickness of soil layers over the bedrock is D. The soil layer is divided into N sublayers with approximately same width. The spatial domains of the sublayers are denoted by D_j, $j = 1, 2, \cdots, N$ while the irregular interfaces are designated by C_i, $i = 1, 2, \cdots, N–1$ (Fig. 2). The boundary between the foundation and the soil layers is considered as Γ. The top free surface is flat and is denoted by S_F. Each irregular interface is assumed to vary around the corresponding flat reference surface with depth z_i, $i = 1, 2, \cdots, N–1$. The flat reference surfaces are denoted by S_i, $i = 1, 2, \cdots, N–1$. If the ith irregular interface is flat, then C_i will coincide with the reference surface S_i. The material properties of the half-space are characterized by shear wave velocity β_R, mass density ρ_R, shear modulus μ_R, and damping ratio ξ_R, while the material properties of the soil layers are characterized by shear-wave velocity β_L, mass density ρ_L, shear modulus μ_L, and damping ratio ξ_L. The radius and mass (per unit length) of the foundation are a and M_0, respectively. The shear wall has width $2a$ and height H with mass M_b per unit length, shear-wave velocity β_b and damping ratio ξ_b. The complex material parameters are denoted by asterisks. The plane S-wave is incident to the soil layer from bedrock by forming an incidence angle θ with horizontal, Fig. 1, and has angular frequency ω. The number N depends on $\omega a/\beta_L$ and as $\omega a/\beta_L$ increases; larger N is needed to ensure accuracy due to the effect of nonlinearity within the soil and different shapes of the soil layers and foundation.

The effective motion of the foundation is represented as a sum of two parts: the response when the inertia of both foundation mass M_0 and shear-wall M_b are not taken into account, and the response associated with the inertial force F_0 of the foundation mass and inertial force F_b of the shear wall. To find the free-field response an indirect boundary integral equation method (Ding

and Dravinski, 1996) is used, which employs Green′s function for the harmonic load in the free-space. Also, results in Liang *et al*. (2013) using Green′s function agree well with the analytical work of Trifunac (1972) for the same model. Therefore we have used the IBEM method, here, with the line load in the foundation surrounded by soil-layers. First the free-field ground motion and scattered wave field in each soil layer is calculated and, accordingly, by adding these two the resultant free-field site motion is found. Then, a set of fictitious distributed harmonic loads is applied on the boundary of the foundation bounded by respective soil layers. Using these loads and the rigid condition of the foundation the displacement and traction Green′s function are found. Next, the impedance function (i.e., the force imposed on a massless foundation when it moves with a unit displacement) is calculated. Finally, the first part of the foundation response is obtained by using the impedance function, and the second part is calculated from the equilibrium condition for the foundation. After this the relative shear wall response is calculated which gives the difference between displacement of the top of shear wall and the foundation along with the effect of scattering of SH-waves.

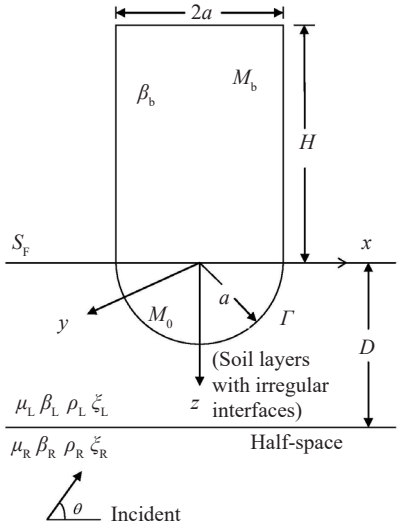

Fig. 1 Model of the problem

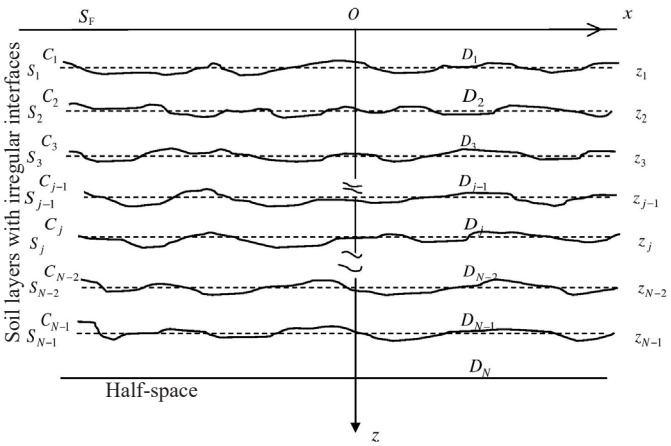

Fig. 2 Soil layers with irregular interfaces in between the half-space and free surface

2.2 Motion of free field

Free-field ground motion is the site response due to the incident SH waves in the absence of the shear wall and foundation. The incident SH wave from the bedrock concerning the displacement is considered in the form of Ding and Dravinski (1996),

$$v^{\text{inc}} = \exp[-\mathrm{i}k_0(x\cos\theta - z\sin\theta) + \mathrm{i}\omega t] \tag{1}$$

in which k_0 is the wave number.

The total wave-field in the multi-layered media can be expressed as a superposition of the wave field due to the flat-layers and scattered wave field according to

$$v_j = v_j^{\text{ff}} + v_j^{\text{s}}, \quad j = 1,\ 2,\ \cdots,\ N \tag{2}$$

in which the superscript ff denotes the wave field of the flat-layer system, and s denotes the scattered wave field caused by the irregular interfaces.

The free-field motion in each flat-layer is given by Ding and Dravinski (1996),

$$\begin{aligned} v_j^{\text{ff}} &= A_j \exp[-\mathrm{i}k_j(x\cos\theta_j - z\sin\theta_j)] + \\ &\quad B_j \exp[-\mathrm{i}k_j(x\cos\theta_j + z\sin\theta_j)]; \\ &\quad (x,z) \in D_j,\ j = 1,2,\cdots,N \end{aligned} \tag{3}$$

where A_j and B_j are amplitudes of the incident and reflected S waves in the domain D_j. The parameters A_j, B_j and θ_j are known from Aki and Richards (1980).

The scattered wave field v^{s} through irregular interfaces of soil layers can be expressed in terms of single-layer potentials per Ding and Dravinski (1996),

$$v_1^{\text{s}} = \sum_{l_j=1}^{L_1} b_{l_1}^1 G_1(\boldsymbol{r},\ \boldsymbol{r}_{l_1});\quad \boldsymbol{r} \in D_1,\quad \boldsymbol{r}_{l_1} \in C_1^+ \tag{4a}$$

$$\begin{aligned} v_j^{\text{s}} &= \sum_{m_{j-1}=1}^{M_{j-1}} a_{m_{j-1}}^j G_j(\boldsymbol{r},\ \boldsymbol{r}_{m_{j-1}}) + \sum_{l_j=1}^{L_j} b_{l_j}^j G_j(\boldsymbol{r},\ \boldsymbol{r}_{l_j}); \\ &\boldsymbol{r} \in D_j;\ j = 2,3,\cdots,N-1;\ \boldsymbol{r}_{m_{j-1}} \in C_{j-1}^-;\ \boldsymbol{r}_{l_j} \in C_j^+ \end{aligned} \tag{4b}$$

$$v_N^{\text{s}} = \sum_{m_1=1}^{M_{N-1}} a_{m_{N-1}}^N G_N(\boldsymbol{r},\ \boldsymbol{r}_{m_{N-1}});\ \boldsymbol{r} \in D_N,\ \boldsymbol{r}_{m_{N-1}} \in C_{N-1}^- \tag{4c}$$

where $a_{m_j}^j$ and $b_{l_j}^j$ denote the sources intensities in the form of amplitudes, r is the position vector of the sources with respect to O, and M_j and L_j represent the order of approximation, that is the number of discretized sources, along the auxiliary surfaces C_j^+ and C_j^- (corresponding to interface C_j), respectively. The functions G_j are Green′s functions for the line load in the free-field which represent the impulsive response, and are given by

$$G_j(r,\ r_0)=\frac{\mathrm{i}}{4}[H_0^2(k_j\sigma_1)+H_0^2(k_j\sigma_2)];\quad j=1,\ 2,\ \cdots,\ N \tag{5a}$$

$$\sigma_1=\sqrt{(x-x_0)^2+(z-z_0)^2}\ ,\quad \sigma_2=\sqrt{(x-x_0)^2+(z+z_0)^2} \tag{5b}$$

in which $H_0^2(\cdot)$ denotes the Hankel function of the second kind and zero order and it is defined as

$$H_0^{(2)}(\cdot)=J_0(\cdot)-\mathrm{i}Y_0(\cdot) \tag{5c}$$

in which $J_0(\cdot)$ and $Y_0(\cdot)$ are Bessel′s function of the first and second kind of zero order respectively.

Putting the values from Eqs. (3) and (4) in Eq. (2) we get the resultant free field motion of the site as

$$\begin{aligned}v_1=&A_1\exp[-\mathrm{i}k_1(x\cos\theta_1-z\sin\theta_1)]+\\&B_1\exp[-\mathrm{i}k_1(x\cos\theta_1+z\sin\theta_1)]+\\&\sum_{l_j=1}^{L_1}b_{l_1}^1\ G_1(r,\ r_{l_1});\ r\in D_1,\ \ r_{l_1}\in C^+\end{aligned} \tag{6a}$$

$$\begin{aligned}v_j=&A_j\exp[-\mathrm{i}k_j(x\cos\theta_j-z\sin\theta_j)]+\\&B_j\exp[-\mathrm{i}k_j(x\cos\theta_j+z\sin\theta_j)]+\\&\sum_{m_{j-1}=1}^{M_{j-1}}a_{m_{j-1}}^j\ G_j(r,\ r_{m_{j-1}})+\ \sum_{l_j=1}^{L_j}b_{l_j}^j\ G_j(r,\ r_{l_j});\\&(x,z)\in D_j,\ \ j=2,3,\cdots,N-1,\\&r\in D_j,\ r_{m_{j-1}}\in C_{j-1}^{-1},\ \ r_{l_j}\in C_j^+\end{aligned} \tag{6b}$$

$$\begin{aligned}v_N=&A_N\exp[-\mathrm{i}k_N(x\cos\theta_N-z\sin\theta_N)]+\\&B_N\exp[-\mathrm{i}k_N(x\cos\theta_N+z\sin\theta_N)]+\\&\sum_{m_1=1}^{M_{N-1}}a_{m_{N-1}}^N\ G_N(r,\ r_{m_{N-1}});\\&r\in D_N,\ r_{m_{N-1}}\in C_{N\text{-}1}^-\end{aligned} \tag{6c}$$

Using the formula of traction i.e., $(\tau_{yz})_j=\mu^*\,\partial v_j/\partial z$ where μ^* modulus of rigidity (Lame coefficient), we can find the tractions from Eq. (6) for different layers as follows.

Traction for the first layer,

$$(\tau_{yz})_1=\mu^*\left[\mathrm{i}k_1\sin\theta_1\ (P_1-P_2)-\frac{1}{4k_1}\sum_{l_1}^{L_1}b_{l_1}^1(P_3+P_4)\right] \tag{7a}$$

where

$$P_1=A_1\exp[-\mathrm{i}k_1(x\cos\theta_1-z\sin\theta_1)] \tag{7b}$$

$$P_2=B_1\exp[-\mathrm{i}k_1(x\cos\theta_1+z\sin\theta_1)] \tag{7c}$$

$$P_3=(z-z_{l_1})\exp[-\mathrm{i}k_1(\sigma_1)_{l_1}]\cdot\frac{\{(\sigma_1)_{l_1}-1\}}{\{(\sigma_1)_{l_1}\}^3} \tag{7d}$$

and,

$$P_4=(z+z_{l_1})\exp[-\mathrm{i}k_1(\sigma_2)_{l_1}]\cdot\frac{\{(\sigma_2)_{l_1}-1\}}{\{(\sigma_2)_{l_1}\}^3};\ z_{l_1}\in C^+ \tag{7e}$$

Traction for the *j*th layer,

$$\begin{aligned}(\tau_{yz})_j=\mu^*[&\mathrm{i}k_j\sin\theta_j\ (Q_1-Q_2)-\\&\frac{1}{4k_j}\sum_{m_{j-1}=1}^{M_{j-1}}a_{m_{j-1}}^j(Q_3+Q_4)\ -\\&\frac{1}{4k_j}\sum_{l_j=1}^{L_j}b_{l_j}^j\ (Q_5+Q_6)]\end{aligned} \tag{8a}$$

where

$$Q_1=A_j\exp[-\mathrm{i}k_j(x\cos\theta_j-z\sin\theta_j)] \tag{8b}$$

$$Q_2=B_j\exp[-\mathrm{i}k_j(x\cos\theta_j+z\sin\theta_j)] \tag{8c}$$

$$Q_3=(z-z_{m_{j-1}})\exp[-\mathrm{i}k_j(\sigma_1)_{m_{j-1}}]\cdot\frac{\{(\sigma_1)_{m_{j-1}}-1\}}{\{(\sigma_1)_{m_{j-1}}\}^3} \tag{8d}$$

$$Q_4=(z+z_{m_{j-1}})\exp[-\mathrm{i}k_j(\sigma_2)_{m_{j-1}}]\cdot\frac{\{(\sigma_2)_{m_{j-1}}-1\}}{\{(\sigma_2)_{m_{j-1}}\}^3} \tag{8e}$$

$$Q_5=(z-z_{l_j})\exp[-\mathrm{i}k_j(\sigma_1)_{l_j}]\cdot\frac{\{(\sigma_1)_{l_j}-1\}}{\{(\sigma_1)_{l_j}\}^3} \tag{8f}$$

$$j=2,\ 3,\cdots,\ N-1.,\ z_{m_{j-1}}\in C_{j-1}^{-1},\ \ z_{l_j}\in C_j^+$$

Traction for the *N*th layer,

$$(\tau_{yz})_N=\mu^*[\mathrm{i}k_N\sin\theta_N\ (R_1-R_2)-\frac{1}{4k_N}\sum_{m_{N-1}=1}^{M_{N-1}}a_{m_{N-1}}^N(R_3+R_4)\ ] \tag{9a}$$

where

$$R_1 = A_N \exp[-\mathrm{i}k_N(x\cos\theta_N - z\sin\theta_N)] \tag{9b}$$

$$R_2 = B_N \exp[-\mathrm{i}k_N(x\cos\theta_N + z\sin\theta_N)] \tag{9c}$$

$$R_3 = (z - z_{m_{N-1}})\exp[-\mathrm{i}k_N(\sigma_1)_{m_{N-1}}]\cdot\frac{\{(\sigma_1)_{m_{N-1}} - 1\}}{\{(\sigma_1)_{m_{N-1}}\}^3} \tag{9d}$$

and

$$R_4 = (z + z_{m_{N-1}})\exp[-\mathrm{i}k_N(\sigma_2)_{m_{N-1}}]\cdot\frac{\{(\sigma_2)_{m_{N-1}} - 1\}}{\{(\sigma_2)_{m_{N-1}}\}^3} \tag{9e}$$

2.3 Motion of foundation with harmonic load

Consider the harmonic line load q_j in the jth sub layer (Fig. 3) of the foundation boundary as (Liang *et al*., 2013)

$$q_j(x,z) = q\delta(z - x\tan\gamma)\exp(\mathrm{i}\omega t) \tag{10}$$

The uniformly distributed line load acting on an inclined line is limited to be within one sub-layer. The time factor $\exp(\mathrm{i}\omega t)$ will be omitted henceforth. Applying inverse Fourier transform to Eq. (10), the line load in wave number domain is obtained as

$$q_j(k',z) = \frac{1}{2\pi}\int_{-\infty}^{\infty} q\delta\ (z - x\tan\gamma)\exp(\mathrm{i}k'x)\mathrm{d}x$$
$$= \frac{q}{2\pi}\exp(\mathrm{i}k'z\cot\gamma) \tag{11}$$

where wave number k' is real valued and is in the range from $-\infty$ to $+\infty$ and is related to θ, ω and β_{R}^* as (Wolf, 1985)

$$k' = \frac{\omega\cos\theta}{\beta_{\mathrm{R}}^*} \tag{12}$$

It has been assumed that the loaded sublayers with the two interfaces are fixed. The calculation of the load on the two interfaces is conducted over local coordinates as in Fig. 3. Accordingly, the dynamic-equilibrium equation for displacement $v(k',z)$ is

$$G_{\mathrm{L}}^*[-k'^2 v(k',z) + v_{,zz}(k',z)] = -\rho_{\mathrm{L}}\omega^2 v(k',z) - q_j(k',z) \tag{13}$$

Physically, Green′s function signifies the impulsive displacement or traction caused by a harmonic load. The displacement Green′s function $g_{u,j}(x,z)$ and traction Green′s functions $g_{t,j}(x,z)$ due to the line load, as in Eq. (11), are per Liang *et al*. (2013)

$$g_{u,j}(x,z) = \int_{-\infty}^{\infty} v\ (k',z)\exp(-\mathrm{i}k'x)\mathrm{d}k' \tag{14}$$

$$g_{t,j}(x,z) = \int_{-\infty}^{\infty} \tau_{yz}(k',z)\exp(-\mathrm{i}k'x)\mathrm{d}k' \tag{15}$$

where

$$v\ (k',z) = v^{\mathrm{p}}(k',z) + v^{\mathrm{h}} \tag{16}$$

Moreover, the term $v^{\mathrm{p}}(k',z)$ involved in Eq. (16) is the particular solution of Eq. (13) which can be expressed per Liang *et al*. (2013) as

$$v^{\mathrm{p}}(k',z) = \frac{q\exp(\mathrm{i}k'z\cot\gamma)}{2\pi\mu_{\mathrm{L}}^* k'^2(\cot^2\gamma - t_{\mathrm{L}}^2)} \tag{17}$$

in which

$$t_{\mathrm{L}} = -\mathrm{i}\sqrt{1 - \frac{1}{m_{\mathrm{L}}^2}},\ m_{\mathrm{L}} = \frac{\beta_{\mathrm{L}}^* k'}{\omega} \tag{18}$$

and γ is the angle between line load and horizontal surface (Fig. 3); for v^{h} (homogeneous solution of Eq. (13)), the calculation is similar to the steps of the calculation of the free-field ground motion as in Eq. (6) c.f. Liang *et al*. (2013).

Also $\tau_{yz}\ (k',z)$ present in the traction Green′s function (Eq. (15)), is expressed as Liang *et al*. (2013)

$$\tau_{yz}\ (k',z) = \tau_{yz}^{\mathrm{p}}\ (k',z) + \tau_{yz}^{\mathrm{h}}(k',z) \tag{19}$$

where

$$\tau_{yz}^{\mathrm{p}}\ (k',z) = \frac{\mathrm{i}qk'\mu\cot\gamma\exp(\mathrm{i}k'z\cot\gamma)}{2\pi\mu_{\mathrm{L}}^* k'^2(\cot^2\gamma - t_{\mathrm{L}}^2)} \tag{20}$$

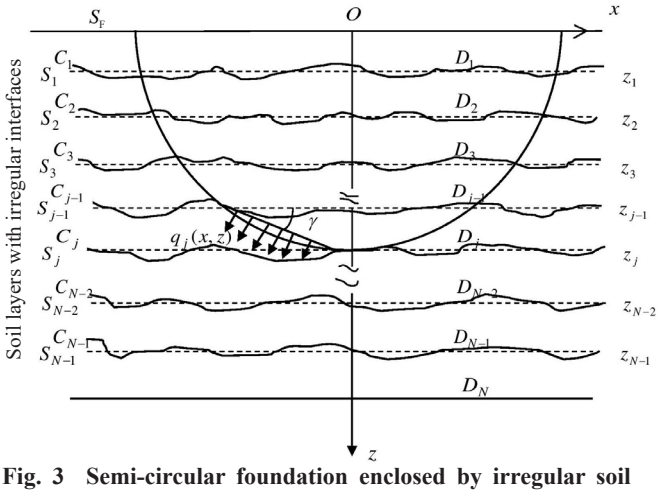

Fig. 3 Semi-circular foundation enclosed by irregular soil layers with distributed load acting on an inclined line

is the particular traction function and $\tau_{yz}^{\mathrm{h}}(k',z)$, the homogeneous traction function, is given by the expressions in Eqs. (7), (8) and (9) but A_j and B_j are evaluated as in Liang *et al*. (2013).

2.4 Impedance function

Impedance function relates the force applied on the massless foundation to the displacement it has caused. If the set of fictitious load q_j $(j=1,2,3,\cdots,N)$ is applied on the surface of the boundary of the foundation Γ, shown in Fig. 3, then the displacement $U(x,z)$ and stress $T(x,z)$ at a point (x,z) on Γ can be expressed per Liang *et al*. (2013) as

$$U(x,z)=\sum_{i=1}^{N} g_{u,j}(x,z)\ q_j,\quad (x,z)\in\Gamma \tag{21}$$

and

$$T(x,z)=\sum_{j=1}^{N} g_{t,j}(x,z)\ q_j,\quad (x,z)\in\Gamma \tag{22}$$

For out of plane excitation, the foundation has out of plane displacement Δ only, where

$$U(x,z)=\sum_{i=1}^{N} g_{u,j}(x,z)\ q_j=\Delta \tag{23}$$

The impedance function relating the force applied on a massless foundation to the displacement is, per Liang *et al*. (2013),

$$K_{yy}=\int_{\Gamma}\sum_{j=1}^{N} g_{t,j}(x,z)\ \Lambda_j \mathrm{d}s \tag{24}$$

where Λ_j are fictitious loads in the jth sub layer when the foundation moves with a unit displacement. Further details about the calculation of impedance function above can be found in Liang *et al*. (2013).

2.5 Effective input motion

The effective displacement response is the response when the site is considered without foundation and wall plus the response when the site is with wall and foundation. If Δ_1 is the motion of the free site and Δ_2 is the motion associated with inertial force F_0 of the foundation mass and inertial force F_{b} of the shear wall then the effective displacement response is

$$\Delta=\Delta_1+\Delta_2 \tag{25}$$

For embedded foundation (Liang *et al*., 2013)

$$\Delta_1=\frac{\int_{\Gamma}\left[U_{\mathrm{f}}(x,z)\sum_{j=1}^{N} g_{t,j}(x,z)\Lambda_j-T_{\mathrm{f}}(x,z)\right]\mathrm{d}s}{K_{yy}} \tag{26}$$

where $U_{\mathrm{f}}(x,z)$ and $T_{\mathrm{f}}(x,z)$ are the displacement and traction of free-field ground motion on boundary Γ respectively given by Eqs. (21) and (22).

Next the displacement Δ_2 caused by the inertial force is

$$\Delta_2=\frac{F_0+F_{\mathrm{b}}}{K_{yy}} \tag{27}$$

where for rigid foundation (Liang *et al*., 2013)

$$F_0=\omega^2 M_0\Delta \tag{28a}$$

Also for shear wall according to Trifunac (1972) and Wolf (1985)

$$F_{\mathrm{b}}=\omega^2 M_{\mathrm{b}}\frac{\tan k_{\mathrm{b}}^{*}H}{k_{\mathrm{b}}^{*}H}\Delta \tag{28b}$$

where $k_{\mathrm{b}}^{*}=\dfrac{\omega}{\beta_{\mathrm{b}}^{*}}$ is the complex wave number in the shear wall.

Substituting the expressions from Eqs. (27), (28a) and (28b) in Eq. (25) we obtain

$$\Delta=\frac{\Delta_1}{1-\dfrac{\omega^2}{K_{yy}}\left[M_0+M_{\mathrm{b}}\dfrac{\tan k_{\mathrm{b}}^{*}H}{k_{\mathrm{b}}^{*}H}\right]} \tag{29}$$

The relative displacement Δ_{b} between the top of the shear wall and the foundation can be written as (Trifunac, 1972)

$$\Delta_{\mathrm{b}}=\Delta\left(\frac{1}{\cos k_{\mathrm{b}}^{*}H}-1\right) \tag{30}$$

In the present paper we have considered the irregular interfaces of soil layers; therefore it will lead the scattering of the incident waves. Accordingly, the displacement response of foundation and shear wall will depend upon the material and physical properties of the system including scattered waves in soil layers. Therefore, to see the effect of scattering of plane waves on the structure response we compare our results with those in the homogeneous half-space (Trifunac, 1972) and soil layers with regular interfaces (Liang *et al*., 2013). For this both Δ and Δ_{b} are normalized by the surface displacement amplitude of free-field ground motion, that is

$$\bar{\Delta}=\frac{\Delta}{|U_{\mathrm{f}}|} \tag{31}$$

$$\bar{\Delta}_{\mathrm{b}}=\frac{\Delta_{\mathrm{b}}}{|U_{\mathrm{f}}|} \tag{32}$$

3 Numerical results and discussion

The results found in this paper for the impedance function, foundation response and relative shear wall response are compared with the existing ones to see the effect of scattered SH waves. For the computation soil parameters of Hollywood Storage Buildings are considered (Fig. 4) (Ding and Dravinski, 1996), and in order to achieve best accuracy of the results, $N = 36$ (number of soil layers) per wavelength is used (Ding and Dravinski, 1996).

A comparison of impedance function is done with the same model embedded in layered viscoelastic half-space (de Barros and Luco, 1995) and in soil layers with regular interfaces (Liang. *et al*., 2013). The expression for the impedance function discussed in (Barros and Luco, 1995) is

$$K_{yy} = \pi\left(\frac{\omega a}{\beta_{\mathrm{L}}}\right)\frac{H_1^{(2)}(\omega a/\beta_{\mathrm{L}})}{H_0^{(2)}(\omega a/\beta_{\mathrm{L}})} \tag{33}$$

where $H_n^{(2)}(\cdot)$ is the Hankel function. Impedance function K_{yy} is normalized by the shear modulus of soil layer μ_{L}. In Eq. (33) $\mathrm{Re}(K_{yy})$ is designated as a normalized stiffness coefficient and $\mathrm{Im}(K_{yy})/(\omega a/\beta_{\mathrm{L}})$ is referred as a normalized damping coefficient.

Figure 5 shows a comparison of our result by means of the solution in (Barros and Luco, 1995; Liang *et al*., 2013) with respect to the dimensionless parameter $\omega a/\beta_{\mathrm{L}}$. It is considered that soil layers and bedrock have identical material properties and the damping ratio 0.0001. Observing the graph, it is seen that the nature of the variation of the real as well as imaginary parts of the impedance function in our result is approximately the same as that of Barros and Luco (1995) and Liang *et al*., (2013). But for the higher values of frequency our result fluctuates with some varying magnitude. The reason behind this is that in our case we have considered the soil layers with irregular interfaces, and the irregularity causes arbitrary scattering for different frequencies of SH waves. In Fig. 6 there is a comparison of foundation response $|\bar{\Delta}|$ in our case with those of Liang *et al*. (2013) and Trifunac (1972), which is

$$|\bar{\Delta}| = \frac{J_1(\omega a/\beta_{\mathrm{L}}) - \dfrac{J_0(\omega a/\beta_{\mathrm{L}})H_1^{(2)}(\omega a/\beta_{\mathrm{L}})}{H_0^{(2)}(\omega a/\beta_{\mathrm{L}})}}{\dfrac{\omega a}{2\beta_{\mathrm{L}}}\left(\dfrac{M_{\mathrm{o}}}{M_{\mathrm{s}}} + \dfrac{M_{\mathrm{b}}}{M_{\mathrm{s}}}\dfrac{\tan(\omega H/\beta_{\mathrm{b}})}{\omega H/\beta_{\mathrm{b}}}\right) - \dfrac{H_1^{(2)}(\omega a/\beta_{\mathrm{L}})}{H_0^{(2)}(\omega a/\beta_{\mathrm{L}})}} \tag{34}$$

We plotted dynamic response of foundation versus the dimensionless parameter $\omega a/\beta_{\mathrm{L}}$ for different values of the parameters $M_{\mathrm{o}}/M_{\mathrm{s}} = 1$ and $M_{\mathrm{b}}/M_{\mathrm{o}} = 1,\ 2,\ 4$. It is seen that the results of the two methods agree very well with some fluctuations for lower frequency which signifies that the scattered waves have high intensity for the lower frequency. This indicates that the resonance of the foundation shifts towards the lower frequency. Moreover it is observed that on increasing the mass of the shear wall amplitude of the foundation response increases.

Scattering of wave is the physical phenomena in which the path of the propagating wave deviates from its original path because of the localized non-uniformities

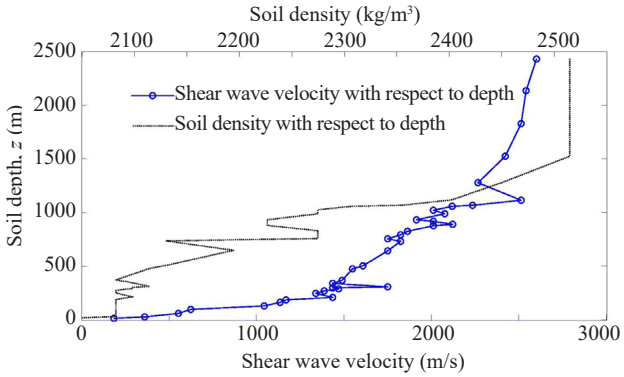

Fig. 4 Soil parameters of the site of the Hollywood Storage Building (Duke *et al*., 1970)

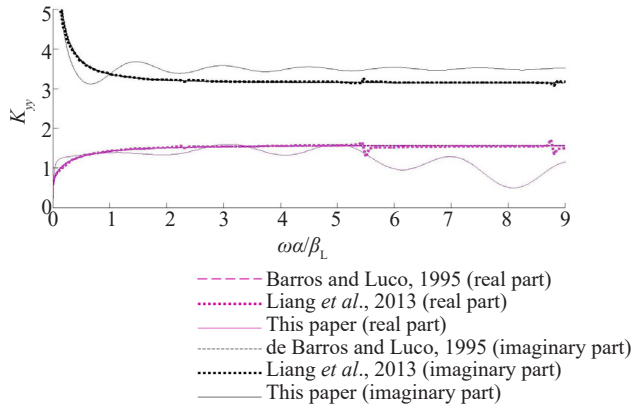

Fig. 5 Effect of scattering of SH waves on impedance function and comparison with those of de Barros and Luco (1995) and Liang *et al*. (2013)

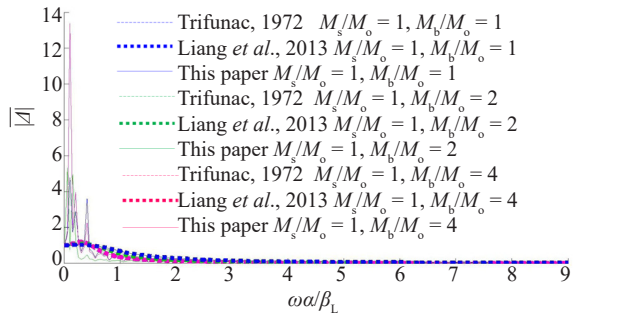

Fig. 6 Effect of scattering of SH waves in foundation response and a comparison with those of Trifunac (1972) and Liang *et al*. (2013)

in the medium. This depends on the number of irregular points on the layers, material properties of the medium, frequency, and the velocity of the wave. To analyze the phenomenon of scattering due to the presence ofirregular points in the soil layers a geometrical model is depicted in Fig. 7. The roughness of the soil layer depends on the irregular points and on increasing the number of irregular points roughness of the layer also increases. The interface between the layer and the half-space is cosine-shaped and is defined by Ding and Dravinski (1996).

$$z=\begin{cases}1, & |x|>0.5\\ 1+0.05(1+\cos 2\pi x), & |x|\le 0.5\end{cases} \tag{35}$$

In Fig. 7, M and L are the number of sources along the auxiliary surfaces C^+ and C^- respectively. Along the interface, the number of collocation points is taken to be N_0. The length of the interface on which the collocation points are distributed is considered as X_n. The sources of lengths X_m and X_l are distributed over the auxiliary surfaces C^- and C^+, respectively; length of the irregular part of the interface is taken to be X_1.

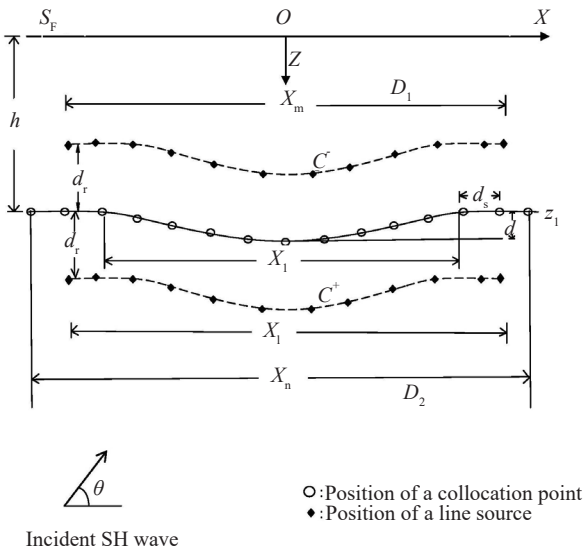

Fig. 7 Geometry of the irregular (i.e., scattering) points in one-layer with a cosine shaped interface

Table 1 Three different sets of irregular points with geometrical values $X_n = 2$, $X_1 = 2.1$, $X_m = 2.1$, $X_1 = 1.9$, $d_s = 0.0339$, $d_r = 3d_s$ and $d = 0.1$ in one layer model

	M	L	N_0	z_1
1st set of irregular points	12	12	30	0.5
2nd set of irregular points	14	14	35	0.6
3rd set of irregular points	16	16	40	0.7

The depth of the flat layer is z_1 and the maximum deviation of the irregular interface from a flat layer is considered as d. The distance between two adjacent collocation points is denoted by d_s Moreover, d_r is the distance between the auxiliary surfaces $C^{\pm}$ and the interface C. Further details about the significance of the considered geometry of the soil layer can be found in Ding and Dravinski (1996).

To see the effect of scattering through the scattering sources in the soil layers we have considered three different set of coordinates (Table 1) demonstrating the position of the irregular points in the soil layers.

Accordingly, Figs. 8 and 9 show that both the foundation response and relative shear wall vibrations are different for the three different respective sets of scattering centers. This indicates that roughness in the soil layers plays an important role in providing the source intensity to the wave passing over it.

Following Trifunac (1972) and Liang *et al*. (2013), we combine the stiffness and the height of the shear wall into a dimensionless parameter $\varepsilon=\beta_L H/\beta_b a$. Then $\varepsilon=0$ corresponds to a rigid shear wall added as a rigid mass to the foundation. Figures 10-14 show the dynamic response of the foundation $|\bar{\Delta}|$ and relative response of shear wall $|\bar{\Delta}_b|$ plotted with respect to the excitation frequency, for different shear wall stiffness ($\varepsilon=0,\ 2,\ 4$), different collective soil-layers thickness relative to the foundation size ($D/a=2,\ 3,\ 4$), different ratio between bedrock and soil layer velocity $(\beta_R/\beta_L=2,\ 4,\ 8)$ and different shear wall masses relative to that of the

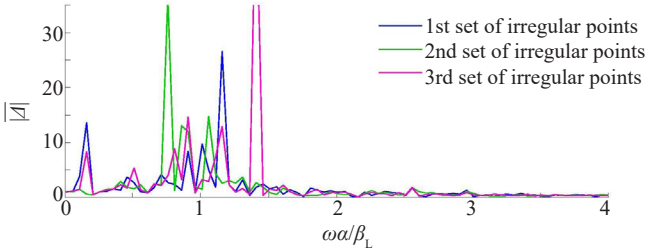

Fig. 8 Effect of scattering of SH waves in foundation due to three different sets of coordinates of irregular points in soil-layers and their respective source intensities

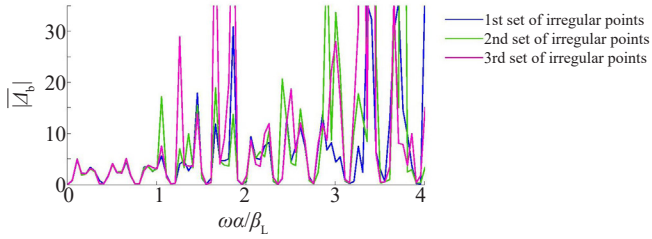

Fig. 9 Effect of scattering of SH waves in the relative shear wall response due to three different sets of coordinates of irregular points in soil-layers and their respective source intensities

foundation $(M_b/M_o = 1, 2)$. For the layered half-space, the parameters are $\rho_R/\rho_L = 1$, $\xi_R = \xi_L = 0.005$ and $\xi_b = 0$. In the layered half-space, the frequency for which interference produces the maximum response of the soil layers is

$$\omega_L = \frac{(2n+1)\pi\beta_L}{2D};\ n = 0, 1, 2, \cdots \qquad (36)$$

Therefore, $D/a = 2$ corresponds to $\omega_L a/\beta_L = 0.79$, 2.36, 3.93, 5.49,…; $D/a = 3$ corresponds to $\omega_L a/\beta_L =$ 0.52, 1.57, 2.62, 3.67,…; $D/a = 4$ corresponds to $\omega_L a/\beta_L = 0.39$, 1.18, 1.96,…; and so on. The resonant frequencies of the shear wall are

$$\omega_b = \frac{(2n+1)\pi\beta_b}{2H};\ n = 0, 1, 2, \cdots \qquad (37)$$

Here, $\varepsilon = 2$ gives $\omega_b a/\beta_L = 0.79$, 2.36, 3.93, 5.49, …; $\varepsilon = 4$ gives $\omega_b a/\beta_L =$ 0.39, 1.18, 1.96, 2.75, 3.53, 4.32, 5.11, …; and so on.

If an incident wave with the above values of frequencies (Eqs. (36) or (37)) passes through the soil layers or shear wall then it produces maximum displacement on the respective mediums. To investigate this phenomenon, frequency of the incident wave is comprised in the expression $\omega a/\beta_L$, and throughout the soil layer it takes the value of $\omega_L a/\beta_L$ for resonant frequency; again on the shear wall, for resonant frequency it takes the value of $\omega_b a/\beta_L$. Resonance of the mediums has been analyzed along with the effect of scattering in the vibrating system.

From the Figs. 10-12 it can be observed that the foundations as well as the relative shear wall response are arbitrary. For different values of the frequency they have different amplitude of vibration. Comprising the scattering of waves among different thickness of the soil layers D, in comparison to radius of the foundation, has significant effects on the dynamics of the system. It can be seen that for higher value of D/a the response

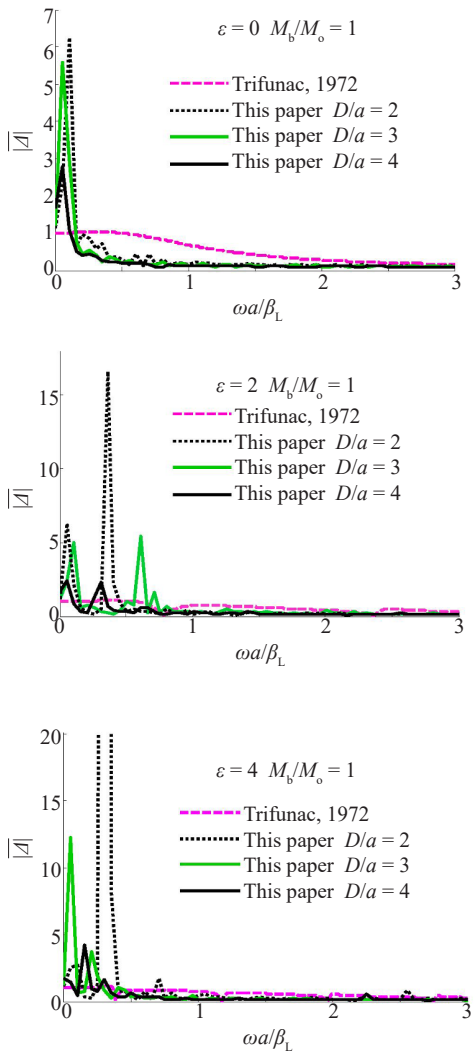

Fig. 10 Dynamic response of foundation for different soil-layer thickness when $\varepsilon = 0$, 2, 4 and $M_b/M_o = 1$

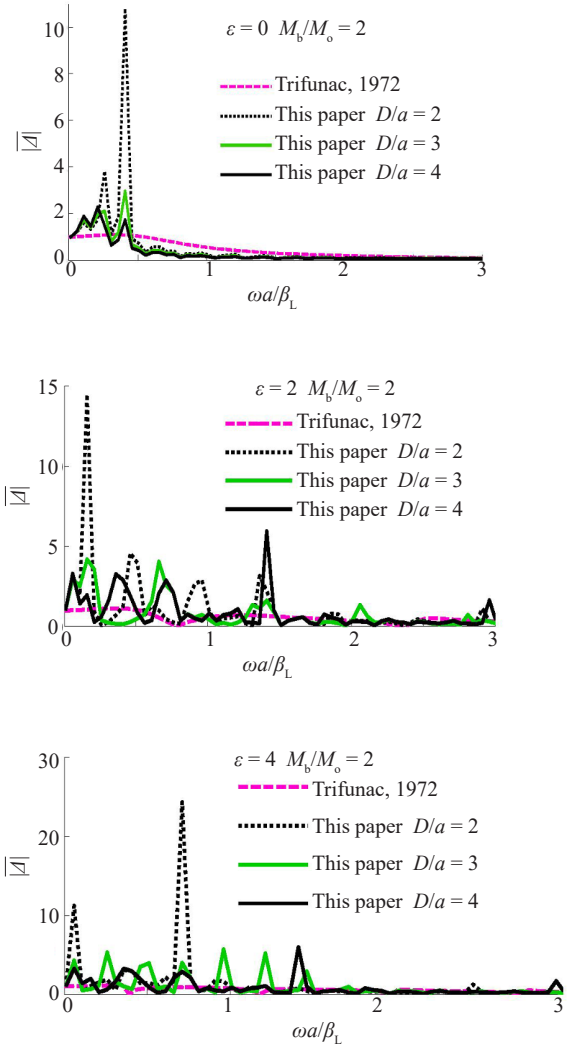

Fig. 11 Dynamic response of foundation for different soil-layer thickness when $\varepsilon = 0$, 2, 4 and $M_b/M_o = 2$

amplitude of the foundation as well as shear wall is low. This signifies that increasing total thickness of the soil-layers in between the bedrock and free surface will lead the small amplitude vibration of the foundation and shear wall. With increasing shear-wall mass (M_b/M_o), the foundation responses around the frequencies at which the soil layers experience the strongest interference increase significantly, implying that a heavier shear wall may go for a larger foundation response. Moreover, it can be seen that with increasing shear-wall flexibility (ε), the peak of the foundation response becomes larger.

Again, increasing the velocity β_R of the wave on the bedrock in comparison to that of layered space β_L has significant effects on the movement of the foundation and relatively in shear wall along with scattering of waves. In Figs. 13 and 14 it is seen that for high value of ratio β_R/β_L the displacement amplitude is high for both foundation and shear wall but again the nature of vibration is arbitrary because of scattering. This shows that increasing relative bedrock stiffness (β_R/β_L) results in the larger foundation response. This can be explained physically by the that larger fraction of wave energy being trapped in the soil layers when (β_R/β_L) increases.

Investigation was also carried out to see the impact of variation in the angle of incidence of SH wave. For this, angle of incidence θ has been considered with

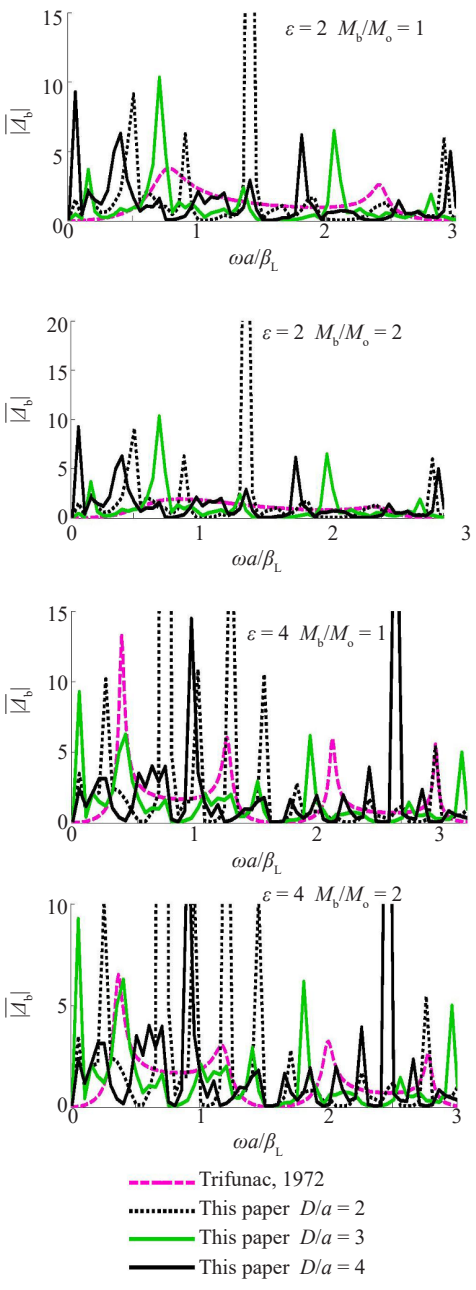

Fig. 12 Relative responses of shear wall for different thickness of soil layer when $\varepsilon = 2, 4$ and $M_b/M_o = 1, 2$

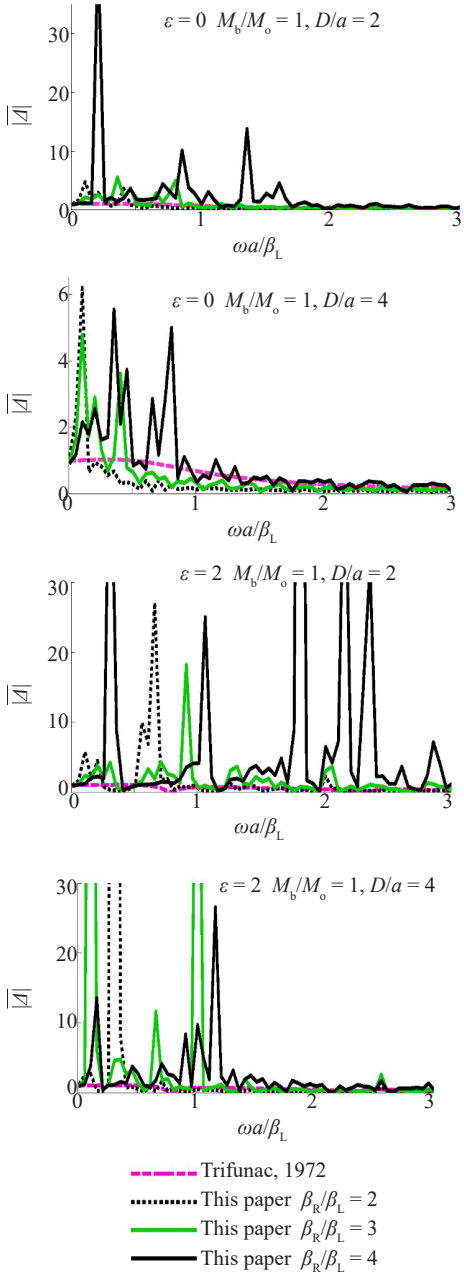

Fig. 13 Dynamic response of foundation for different SH wave velocities in half-space relative to soil layers when $\varepsilon = 0, 2$ and $M_b/M_o = 1$ and $D/a = 2, 4$

the values $\theta = \pi/2, \pi/3, \pi/4, \pi/9$. From Figs. 15 and 16 it is observed that for the vertically incident waves ($\theta = \pi/2$) the scattering is taking place in large scale and displacement of both the foundation and shear wall is high. At the same time it is observed that if the wave is striking the system with some angle of inclination ($\theta = \pi/3, \pi/4, \pi/9$) then the scattering magnitude is low, and as well the displacement response varies in small scale.

Finally, it is seen that due to scattered S waves in soil layers the dynamic response of the foundation and shear wall fluctuates around the analytical result for the same model. In general, for larger bedrock stiffness $\beta_R/\beta_L = 4, 8$ as the shear wall flexibility ε increases the largest peaks of the foundation response gradually shift toward lower frequencies, indicating that the system becomes more flexible. Increasing shear-wall mass M_b/M_o, collective soil-layer thickness D/a and bedrock stiffness β_R/β_L all influence the dynamics of the foundation and shear wall. This indicates that there exists interaction between the shear wall and the soil layers with scattering of SH waves.

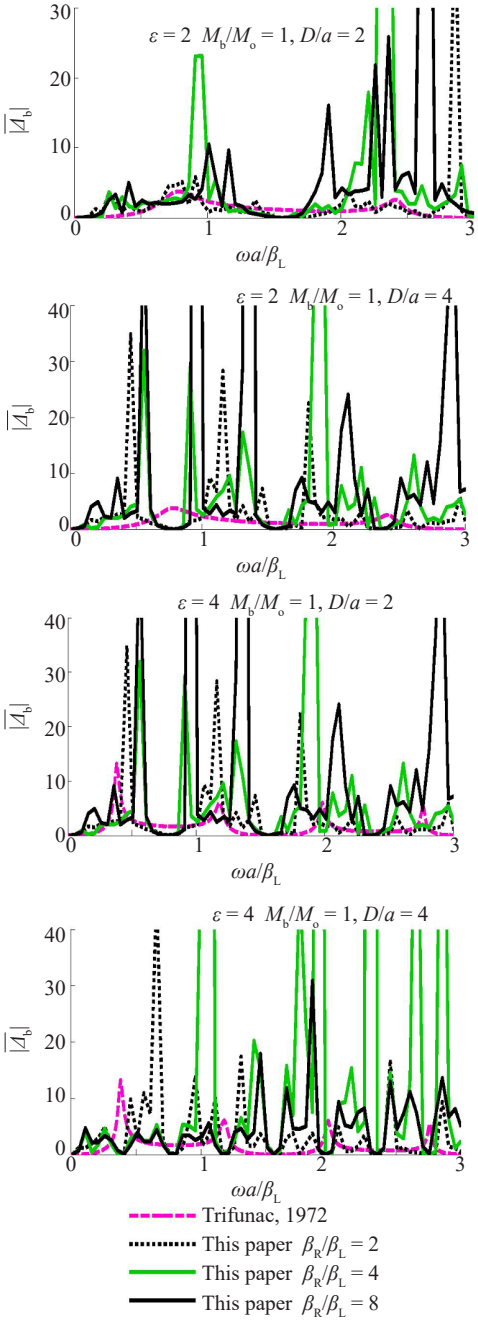

Fig. 14 Relative response of shear-wall for different SH wave velocity in half-space relative to soil layers when $\varepsilon = 2, 4$ and $M_b/M_o = 1$ and $D/a = 2, 4$

4 Conclusions

In the present assignment, the outcome of the dynamic soil-structure interaction, using the composite model consisting of shear-wall with semi-circular foundation embedded in the soil-layers with irregular faces, has been investigated by implementing indirect boundary element method (IBEM). Displacement of the model consisting of shear wall with foundation is evaluated using the Green′s function of line load in the free space and foundation. The expressions for the dynamic response of model contain the terms signifying the scattering of waves through soil layers. Moreover, to see the effect of roughed interfaces of soil-layers a comparison was made with the analytical solutions and showed that both the foundation response and the shear wall movement have arbitrary nature of vibration due to scattering, but their amplitudes fluctuate around the responses of the analytical results. This varying nature of displacement is arbitrary and is included in both the dynamics of foundation and shear wall. It is seen that the physical properties of the layered soil, bedrock and the shear wall are effective for the vibrant response

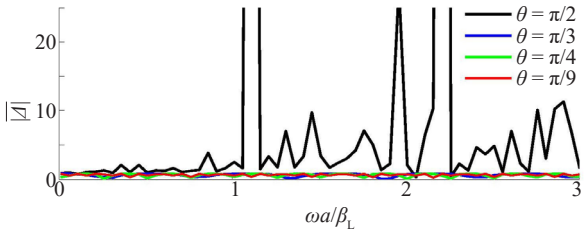

Fig. 15 Response of foundation for different angles of incidence of SH waves taking $\varepsilon = 3$ and $M_b/M_o = 2$ and $D/a = 2$

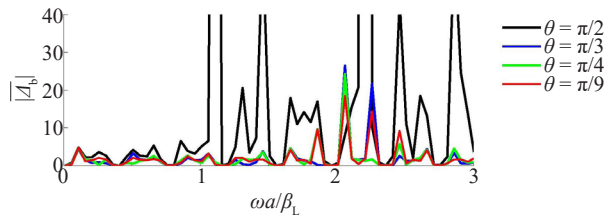

Fig. 16 Response of shear wall for different angles of incidence of SH wave taking $\varepsilon = 3$ and $M_b/M_o = 2$ and $D/a = 2$

of the system and soil-structure interaction. Particularly, the media between the bedrock and free space has a predominant role in the soil-structure interaction. Half-space stiffness, soil-layer thickness, irregularity of soil-layers, shear wall stiffness and shear-wall mass all affect the dynamics of foundation and relative shear wall response.

Acknowledgement

We would like to express our sincere appreciation to the Department of Mathematics, Birla Institute of Technology, Mesra, Ranchi, India for providing the research facility and allied supports while preparing this research paper. We are also thankful to Cambridge Institute of Technology, Ranchi, India for providing the allied support while the revision of this paper was conducted. Moreover, we are indebted to the reviewers whose comments and suggestion leads to significant improvement in this manuscript.

References

Abascal R and Dominguez J (1986), "Vibrations of Footings on Zoned Viscoelastic Soils," *Journal of the Engineering Mechanics Division*, *ASCE*, **112**(5): 433–447.

Aki K and Richards PG (1980), *Quantitative Seismology, Theory and Methods*, Vol. 1, W. H. Freeman, San Francisco, USA.

Apsel RJ and Luco JE (1976), "Torsional Response of Rigid Embedded Foundation," *Journal of the Engineering Mechanics Division, ASCE*, **102**(6): 957–970.

Ba Z, Kang Z and Liang J (2018), "In-Plane Dynamic Green′s Functions for Inclined and Uniformly Distributed Loads in a Multi-Layered Transversely Isotropic Half-Space," *Earthquake Engineering and Engineering Vibration*, **17**(2): 293–309.

Clayton R and Engquist B (1977), "Absorbing Boundary Conditions for Acoustic and Elastic Wave Equations," *Bulletin of the Seismological Society of America*, **67**(6): 1529–1540.

de Barros FCP and Luco JE (1995), "Dynamic Response of a Two-Dimensional Semi-Circular Foundation Embedded in a Layered Viscoelastic Half-Space," *Soil Dynamics & Earthquake Engineering*, **14**(1): 45–57.

Ding G and Dravinski M (1996), "Scattering of SH Waves in Multilayered Media with Irregular Interfaces," *Earthquake Engineering and Structural Dynamics*, **25**(12): 1391–1404.

Duke CM, Luco JE, Carriveau AR, Hradilex PJ, Lastrico R and Ostrom D (1970), "Strong Earthquake Motion and Site Conditions: Hollywood," *Bulletin of the Seismological Society of America*, **60**(4): 1271–1289.

Engquist B and Majda A (1977), "Absorbing Boundary Conditions for the Numerical Simulation of Waves," *Mathematics of Computation*, **31**(139): 629–651.

Higdon RL (1986), "Absorbing Boundary Conditions for Difference Approximations to the Multi Dimensional Wave Equation," *Mathematics of Computation*, **47**(176): 437–459.

Japon BR, Gallego R and Dominguez J (1997), "Dynamic Stiffness of Foundations on Saturated Poroelastic Soils," *Journal of the Engineering Mechanics Division, ASCE*, **123**(11): 1121–1129.

Kausel E, Roesset JM and Waas G (1975), "Dynamic Analysis of Footings on Layered Media," *Journal of the Engineering Mechanics Division, ASCE*, **101**(5): 679–693.

Lee VW (1979), "Investigation of Three Dimensional Soil-Structure Interaction," *Report No. CE 79–11*, Department of Civil Engineering, University of Southern California, Los Angeles.

Lee VW and Luo H (2014), "Soil-Structure Interaction on Shallow Rigid Circular Foundation: Plane SH Waves from Far-Field Earthquakes," *Earthquake Engineering and Engineering Vibration*, **13**(1): 29–45.

Li Jianbo, Liu Jun and Lin Gao (2013), "Dynamic Interaction Numerical Models in the Time Domain Based on the High Performance Scaled Boundary Finite Element Method," *Earthquake Engineering and Engineering Vibration*, **12**(4): 541–546.

Liang J and Ba Z (2007), "Surface Motion of an Alluvial Valley in Layered Half-Space for Incident Plane SH Waves," *Journal of Earthquake Engineering and Engineering Vibration*, **27**(7): 1–9. (in Chinese with English abstract)

Liang J and Ba Z (2008), "Surface Motion of a Hill in Layered Half-Space subjected to Incident Plane SH Waves," *Journal of Earthquake Engineering and Engineering Vibration*, **28**(1): 1–10. (in Chinese with English abstract)

Liang J, Jia F, Todorovska M and Trifunac MD (2013), "Effects of the Site Dynamic Characteristics on Soil–Structure Interaction (I): Incident SH-Waves" *Soil Dynamics and Earthquake Engineering*, **44**: 27–37.

Liao ZP (1999), "Dynamic Interaction of Natural and Man-Made Structures with Earth Medium," *Earthquake Research in China*, **11**(7): 367–408.

Liao ZP, Wong HL and Yang B (1984), "A Transmitting Boundary for Transient Wave Analyses," *Science in China*, *Series A*, **17**(11): 1063–1076.

Luco JE (1969), "Dynamic Interaction of a Shear Wall with the Soil," *Journal of the Engineering Mechanics Division, ASCE*, **95**(2): 333–346.

Luco JE (1976), "Torsional Response of Structures for SH Waves: the Case of Hemispherical Foundation," *Bulletin of the Seismological Society of America*, **66**(1): 109–123.

Luco JE and Wong HL (1987), "Seismic Response of Foundations Embedded in a Layered Half-Space," *Earthquake Engineering & Structural Dynamics*, **15**: 233–247.

Manolis GD and Beskos DE (1988), "Boundary Element Methods in Elastodynamics," *London: Chapman & Hall*, Chapter 6.

Messioud S, Sbartai B and Dias D (2016), "Seismic Response of a Rigid Foundation Embedded in a Viscoelastic Soil by Taking into Account the Soil-Foundation Interaction," *Structural Engineering and Mechanics*, **58**(5): 887–903.

Sbartai B and Boumekik A (2008), "Ground Vibration from Rigid Foundation by BEM-TLM," *ISET Journal of Earthquake Technology*, **45**(3-4): 65–78.

Smith WD (1974), "A Nonreflecting Plane Boundary for Wave Propagation Problems," *Journal of Computational Physics*, **15**(4): 492–503.

Tassoulas JL and Kausel E (1983), "On the Effect of the Rigid Sidewall on the Dynamic Stiffness of Embedded Circular Footings," *Earthquake Engineering & Structural Dynamics*, **11**: 403–414.

Todorovska MI (1993), "In-Plane Foundation-Soil Interaction for Embedded Circular Foundations," *Soil Dynamics and Earthquake Engineering*, **12**(5): 283–297.

Todorovska MI and Rjoub YA (2006a), "Effect of Rainfall on Soil-Structure System Frequency: Examples based on Poroelasticity and a Comparison with Full-Scale Measurements," *Soil Dynamics and Earthquake Engineering*, **26**(6-7): 708–717.

Todorovska MI and Rjoub YA (2006b), "Plain Strain Soil-Structure Interaction Model for a Building Supported by a Circular Foundation in a Poroelastic Half-Space," *Soil Dynamics and Earthquake Engineering*, **26**(6-7): 694–707.

Trifunac MD (1972), "Interaction of a Shear Wall with the Soil for Incident Plane SH Waves," *Bulletin of the Seismological Society of America*, **62**(1): 63–83.

Wang F, Tao X, Xie L and Siddharthan R (2017), "Green′s Function of Multi-Layered Poroelastic Half-Space for Models of Ground Vibration due to Railway Traffic," *Earthquake Engineering and Engineering Vibration*, **16**(2): 311–328.

Wolf JP (1985), *Dynamic Soil–Structure Interaction*, Englewood Cliffs, NJ: Prentice- Hall.

Wolf JP and Darbre GR (1984a), "Dynamic-Stiffness Matrix of Soil by the Boundary- Element Method: Conceptional Aspects," *Earthquake Engineering & Structural Dynamics*, **12**(3): 385–400.

Wolf JP and Darbre GR (1984b), "Dynamic-Stiffness Matrix of Soil by the Boundary-Element Method: Embedded Foundation," *Earthquake Engineering & Structural Dynamics*, **12**(3): 401–416.

Wong HL and Trifunac MD (1974), "Interaction of a Shear Wall with the Soil for Incident Plane SH Waves: Elliptical Rigid Foundation," *Bulletin of the Seismological Society of America*, **64**(6): 1825–1842.